Isentropic Analysis applied to Convection, Hurricanes and Walker Circulation

Olivier Pauluis, Agnieszka Mrowiec, Joanna Slawinska,
and Fuqing Zhang

Northeast Tropical Conference, May 27 2013

1 Introduction

In atmospheric convection the ascent of warm, moist air in saturated turbulent plumes is balanced by a subsidence of dryer and colder air in the environment or in convective or mesoscale downdrafts. Convective systems are associated with a variety of turbulent motions over a wide range of scales. Any analysis of such flow is difficult because individual air parcels undergo multiple dynamical and thermodynamical transformations. Moreover, the assessment of the convective processes in complex numerical simulations is based on limited number of dynamical and thermodynamical variables, and because models use different parameterizations and direct comparison without detailed knowledge of any particular model is not always possible.

The proposed approach takes advantage of the quasi-conservation of entropy to isolate convective overturning from oscillatory motions. Isentropic coordinates have been, in the past, applied in studies of: moist-conveyor belt [2], moist convection [19], tropical cyclogenesis [18, 9], hurricane intensity [10] and structure [8]. Isentropic analysis has also provided important insights on the global atmospheric circulation. Averaging the velocity on surfaces of constant potential temperature [1, 5, 3] leads to a single Equator-to-Pole overturning cell in each hemisphere (in contrast to the three-cell structure of the Eulerian-mean circulation). Pauluis and Czaja [15, 13] have analyzed the mean meridional circulation on moist isentropes (surfaces of constant equivalent potential temperature). They show that the circulation on moist isentropes because the large poleward flow of warm moist air supplies water vapor to the stormtracks where it rises into the upper troposphere. This averaging procedure reduces a four-dimensional datasets into a two-dimensional distribution by compressing fluctuations in the two horizontal coordinates and time into a single thermodynamic coordinate.

We present a short description of he isentropic analysis method, followed by three applications in context of numerically resolved convection. First the studies of radiative-convective equilibrium which will be presented by Olivier Pauluis, then the idealized hurricane circulation presented by Agnieszka Mrowiec, and finally the Walker Circulation which will be presented by Joanna Slawinska.

2 Method

Our approach is to compute the conditional average of vertical mass transport in terms of the equivalent potential temperature (similarly to [7]. The mass transport can then be integrated to obtain a streamfunction, which offers a simple representation of the convective overturning. In general, we define the isentropic distribution of the variable f as the integral of a f on a given isentropic surface:

$$\langle f \rangle (z, \theta_{e0}) = \frac{1}{PL_xL_y} \int_0^{L_y} \int_0^{L_x} f(x, y, z, t) \delta(\theta_{e0} - \theta_e(x, y, z, t)) dx\, dy\, dt. \tag{1}$$

θ_e is the equivalent potential temperature, P is the time period over which we average and L_x and L_y are the horizontal size of the domain. The Dirac delta function can be approximated by a function equal to $1/\Delta\theta_e$ for θ_e between $\theta_{e0} - 0.5\Delta\theta_e$ and $\theta_{e0} + 0.5\Delta\theta_e$, and 0 elsewhere. In practice, equation (1) amounts to sorting the air parcels in terms of their equivalent potential temperature and to summing the quantity f at each vertical level in finite θ_e bins. The units of $< f >$ are given by the units of f per degree Kelvin. The isentropic distribution defined by (1) is therefore a function of height and equivalent potential temperature. From now on it should be understood that all isentropic integrals $\langle \cdot \rangle$ are function of both z and θ_e, unless stated otherwise.

The isentropic distribution of the vertical mass flux $\langle \rho w \rangle$ defined with equation (1) has units of (kg m^{-2} s^{-1}K $^{-1}$), corresponding to a vertical mass flux per unit area and per unit of equivalent potential temperature. The quantity $\langle \rho w \rangle \, \delta\theta_e$ corresponds to the net vertical mass flux of air parcels at level z with an equivalent potential temperature between θ_e and $\theta_e + \delta\theta_e$. The isentropic mass flux $\langle \rho w \rangle$ can be then used to define an isentropic streamfunction as follows:

$$\Psi(z, \theta_e) = \int_{-\infty}^{\theta_e} \langle \rho w \rangle (z, \theta'_e) d\theta'_e. \tag{2}$$

From a physical point of view, the streamfunction $\Psi(z, \theta_e)$ can be interpreted as the net vertical mass flow per unit area at level z of all air parcels with an equivalent potential temperature less than θ_e and the mean trajectory of air parcels in the $(z - \theta_e)$ space is along the streamlines.

The isentropic integral in (1) is not limited to vertical mass flux. The same formalism can be applied to any variable of interest to obtain a more detailed analysis of the typical properties of the air parcels involved in convective motions. The probability for finding a parcel with equivalent potential temperature θ_e at level z can be estimated as

$$PDF(z, \theta_e) = \frac{\langle \rho \rangle (z, \theta_e, t)}{\overline{\rho}(z)} \tag{3}$$

The isentropic distributions for the vertical mass flux $\langle \rho w \rangle$ and for density $\langle \rho \rangle$ can be combined to define a horizontal and isentropic mean vertical velocity $\tilde{w}(\theta_e, z)$ for air parcels with a given value of θ_e at level z:

$$\tilde{w}(z, \theta_e) = \frac{\langle \rho w \rangle (z, \theta_e)}{\langle \rho \rangle (z, \theta_e)} \tag{4}$$

The averaging procedure used to define the isentropic mean vertical velocity can be applied to any variable as the mass weighted isentropic mean. This formulation offers an efficient way to characterize the thermodynamic properties of convective overturning.

3 Radiative-convective equilibrium circulation Presented by Olivier Pauluis

The isentropic averaging technique was used to analyze a simulation of radiative-convective equilibrium performed with the System for Atmospheric Modeling (SAM), a Cloud Resolving Model developed by [6]. The model was integrated on 216 km x 216 km x 28 km domain at 500 m horizontal resolution and stretched vertical grid with 64 gridpoints, with periodic boundary conditions in the horizontal directions. The lower boundary is at constant temperature of 301 K, while a sponge layer is applied in the upper 8 km to prevent the reflection of gravity waves. The model uses a 5 species single-moment microphysics, an explicit radiative transfer, and was integrated for 100 days, with the last 60 days used for the time averaging. The isentropic distribution of the the vertical mass flux and the isentropic streamfunction

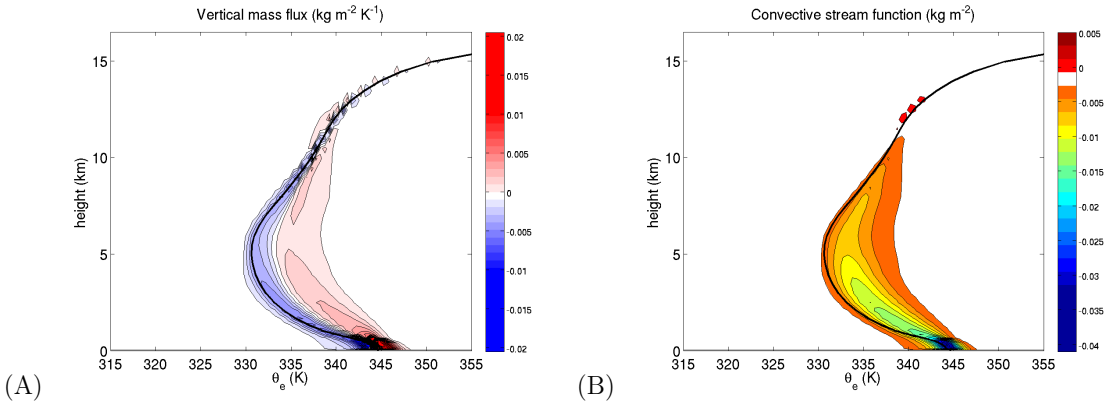

(A) (B)

Figure 1: Left panel: Isentropic distribution of vertical mass flux $\langle \rho w \rangle$ (kg m^{-2} s^{-1} K^{-1}) in the radiative-convective equilibrium simulations. Right panel: Isentropic streamfunction $\Psi(z, \theta_e)$ (kg m^{-2} s^{-1}). The solid line shows the mean profile of equivalent potential temperature $\overline{\theta}_e(z)$.

are shown respectively in Figure 1A and 1B. Given the definition (2), a negative value of the streamfunction through most of the atmosphere indicates that rising air parcels have on average a higher equivalent potential temperature than the subsiding air, and thus corresponds to an upward transport of θ_e. The absolute minimum of the streamfunction is located near the surface and is associated with mixing within the sub-cloud layer. The magnitude of the streamfunction decreases above 1km, then decreases more gradually with height all the way to the tropopause, corresponding to a continuous detrainment of air from the updrafts. The streamfunction changes sign at about 12 km, pointing to the presence of convective overshoots associated with a weak downward entropy and energy transport as rising air mixes with air parcels with higher potential temperature before subsiding.

Ascending air parcels originating from the lowest atmospheric layer have high values of θ_e, up to 355 K. The equivalent potential temperature of the ascending air however drops rapidly with height, indicating entrainment of dryer air in the updrafts. Above 4–5 km the streamlines become almost vertical, corresponding to a vanishing mean diabatic tendency in the updraft, which would indicate that the role of entrainment is limited above the freezing level. As adiabatic freezing or sublimation can lead to an increase in the equivalent potential

temperature, the vertical streamlines above the freezing level might actually be the results of the compensation between freezing and entrainment.

The bulk of the descending motion occurs at equivalent potential temperature close to the horizontal mean atmospheric state. Furthermore, the streamlines are closely alined with the mean profile $\overline{\theta}_e(z)$. The subsiding part of the circulation corresponds to a slow subsidence of air parcels whose equivalent potential temperature remains close to $\overline{\theta}_e(z)$. The minimum value of $\overline{\theta_e}(z)$ is 330 K and is located at 5 km, near the freezing level. Above this minimum, the equivalent potential temperature of the subsiding air decreases as a direct consequence of radiative cooling. In contrast, below the minimum of $\overline{\theta}_e$ the equivalent potential temperature of subsiding air parcels gradually increases as they approach the surface. While radiative cooling is still present, the increase of θ_e is directly tied to the mixing between subsiding environmental air and detrained cloudy air with a higher value of θ_e. Mixing between rising clouds and the surrounding air is associated with a exchange of latent heat from the former to the later. This process can be directly diagnosed by the tilt of the streamfunction in the lower troposphere, which is reflects both in a gradual reduction of the equivalent potential temperature of the ascending air, and a comparable increase of the equivalent potential temperature in subsiding air.

4 Hurricane circulation
Presented by Agnieszka Mrowiec

The Weather Research and Forecasting (WRF 2.2) model was used to produce the idealized hurricane simulations. We analyze the 1000km by 1000km domain at 1km horizontal resolution [17]. There are 35 stretched vertical levels with the top at 28km. In the simulations analyzed in this project both the long-wave and short-wave radiation effects are neglected (like in [12]), the WRF Single-Moment, 6-class scheme with graupel (WSM6) microphysics is used [4], and the turbulent fluxes from Yonsei University (YSU) scheme [11] are applied. The simulations were initialized with an axisymmetric vortex (similar to [16]) located at 20 N with an initial radius of 102 km) and tangential wind $v_t = 16$ m/s.

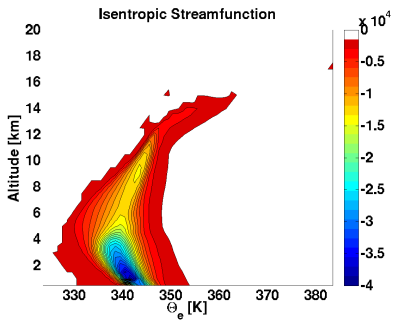

Figure 2: The isentropic streamfunction averaged over the most intense, steady period.

For this study we we chose 12 hours of the most steady, axisymmetric circulation and average the isentropic flow over that period. The motivation was to look at the characteristics of this steady state and compare it later with transient features. In Figure 2 the isentropic streamfunction is shown. For the hurricane circulation, the upward moving portion of the circilation is wide in the θ_e-z space. In particular, the class of ascending air parcels with $\theta_e > 347$ K corresponds to the eyewall. The downward motion happens at the temperatures close to the environmental mean and the downward flow is the strongest below 4 km. Because the the number of air parcels circulating at lower equivalent potential temperature values is much larger than for the eyewall, it is difficult to see the eyewall flow

in this figure. Looking at other properties of the flow helps to solve this problem.

Mass flux at the distance from the center to about 50km (the eye and the eyewall with the adjacent downdraft) is shown in figure Figure 3A. Figure 3B shows the isentropic mass flux for the mesoscale convection extending from about 50km to about 350 km. Beyond 350km (not shown) the flow is dominated by large-scale subsidence.

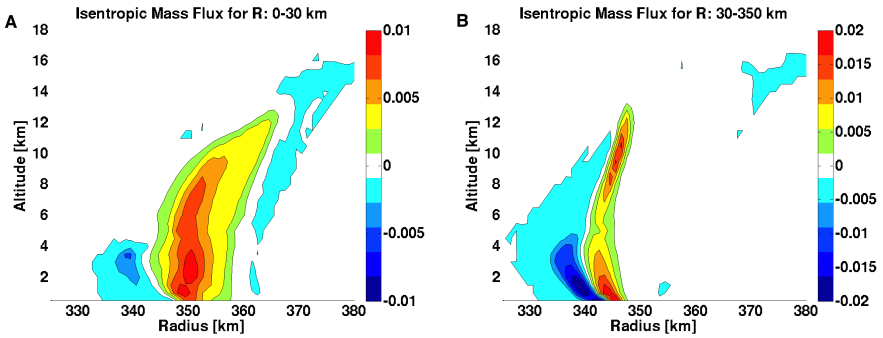

Figure 3: Mass flux for radial interval corresponding to the eye + eyewall and to large scale.

The ascent in the eyewall happens at the equivalent potential temperatures between about 347 K and 360 K. For the temperatures higher than 360 K there is a downward mass transport corresponding to the eye. There are also cooler subsiding parcels outside of the eyewall and below 4 km. For radii further away from the center, the upward mass transport happens at about 345 K and has two maxima, one below 4 km which matches the downward mass flux (which points to a low level overturning circulation), and the upper level maximum connected with a rain band or isolated convective clouds.

A complementary way of describing the hurricane circulation is to sort convective regimes based on the range of equivalent potential temperature. The mass flux for different θ_e intervals is shown: for 348 - 368 K in Figure 4A, 342-347 K Figure 4B, and for 330-340 K in Figure 4C.

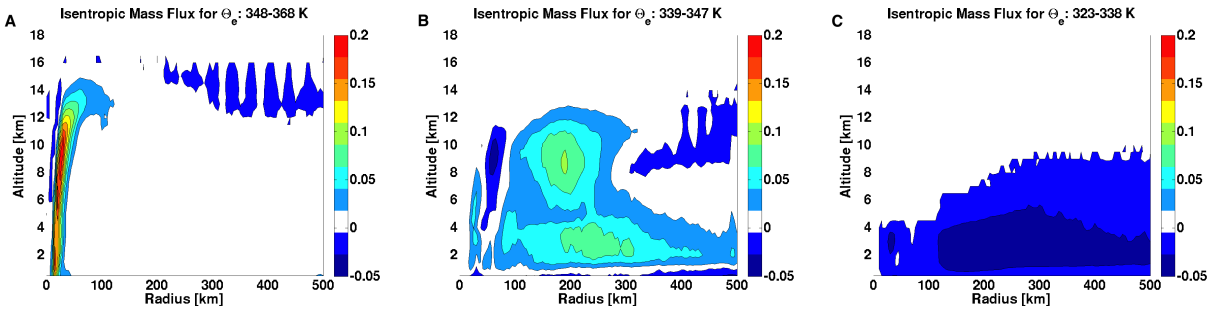

Figure 4: Mass flux averaged over the chosen equivalent potential temperature intervals.

The warmest equivalent potential temperature interval captures the eyewall mass transport. Note that all the air in this case is going up. For the coldest θ_es all the air is transported downward. In the middle regime there are two distinct maxima in the upward mass flux corresponding to the low level overturning and the upper level one, connected with a rain band and large scale upward moving air parcels.

5 Walker circulation
Presented by Joanna Slawinska

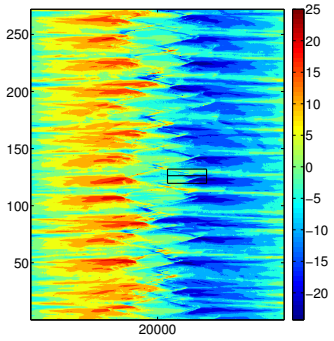

Figure 5: Hovmoller diagram for horizontal velocity (m s1). X axis: x direction (km). Y axis: time (day).

We investigate next the interactions between convection and a planetary scale circulation. For this, we simulate an idealized Walker circulation forced by variations in surface sea temperature (SST). The Walker cell emerges as the time averaged statistical steady state.The circulation exhibits intra-seasonal variability on a time-scale of about 20 days with quasi-periodic intensification of the circulation and broadening of the convective regime. The low frequency oscillation has four main stages: a suppressed stage with strengthened mid-level circulation, intensification phase, active phase with strong upper level circulation and a weakening phase. From a dynamical point of view, the low frequency anomaly exhibits several characteristics of a fluctuation driven by moisture perturbations. In particular, the active phase is proceeded by gradual build up of water content of the atmosphere. As this build-up occurs primarily over the subsidence region, advection of moisture from the subsidence regions to the regions of active precipitation plays an important role in the onset of the active phase.

The impact of convection is crucial for moistening the atmosphere and subsequently large-scale dynamics. Large-scale flow is strongly coupled with synoptic and mesoscale convective systems that emerge frequently. We analyze properties of convection and its organization by applying isentropic streamfunction analysis. In this case, we focus on the scale dependency of the convective streamfunction, by isolating the mass transport associated with the convective, meso, synoptic and planetary scales. It is found that the convective scales account for the bulk of the upward mass transport. However, the contribution of the larger-scale become significant in the upper troposphere.

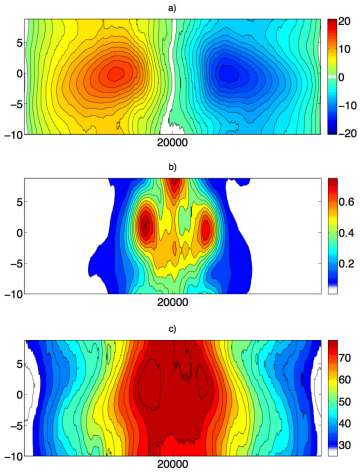

Figure 6: Hovmoller diagram of lag regression of a) surface wind (m s1), b) precipitation (mm h1), c) precipitable water content (kg m2). X axis: x direction (km). Y axis: time (days).

6 Conclusions

A conditional averaging based on equivalent potential temperature has the advantage of preserving the separation between the ascent of warm, moist air and subsidence of colder, dryer air which are the fundamental aspects of moist convection. Furthermore, while the equivalent potential temperature of an air parcel can be affected by a wide range of processes, such radiation, evaporation, and mixing, it is conserved for reversible adiabatic transformation. As defined, isentropic averaging can be viewed as isolating the irreversible convective overturning by

filtering out fast, reversible oscillatory motions (such as gravity
waves), and captures the core convective processes associated with high entropy updrafts balanced by slow subsidence of of low entropy air. By further synthesize the information through mean updraft and a mean downdraft based on the isentropic streamfunction one can describe the mean updrafts and downdrafts properties. The approach presented here is well suited for analysis of simulated convection without requiring detailed knowledge of the numerical models. This can be advantageous in diagnostics of the convective transport in increasingly complex numerical models. While direct computation of the isentropic streamfunction requires a significant amount of data, it might be possible to approximate it accurately on the basis of a statistical approximation, similarly as it can be done using the Statistical Transformed Eulerian-Mean circulation to reconstruct the global isentropic circulation [14]. Hence, the isentropic streamfunction could potentially be used as an intermediary diagnostic for comparison between high resolution cloud resolving models and single column models.

References

[1] J.A. Dutton. *The Ceaseless Wind*. McGraw-Hill, New York, 1976.

[2] T.W. Harrold. Mechanisms influencing the distribution of precipitation within baroclinic structure. *Quart. J. Roy. Meteorol. Soc.* , 99:232–251, 1973.

[3] I. M. Held and T. Schneider. The surface branch of the zonally averaged mass transport circulation in the troposphere. *J. Atmos. Sci.*, 56:1688–1697, 1999.

[4] S.-Y. Hong, J. Dudhia, and S.-H. Chen. A revised approach to ice microphysical processes for the bulk parameterization of clouds and precipitation. *Mon. Weath. Rev.*, 132:103–120, 2004.

[5] D. R. Johnson. The forcing and maintenance of global monsoonal circulations: An isentropic analysis. *Advances in Geophysics*, 31:43–304, 1989.

[6] Marat F. Khairoutdinov and David A. Randall. Cloud resolving modeling of the ARM summer 1997 IOP: Model formulation, results, uncertainties, and sensitivities. *J. Atmos. Sci.*, 60(4):607–625, 2003.

[7] Z. Kuang and C. Bretherton. A mass-flux scheme view of a high-resolution simulation of a transition from shallow to deep cumulus convection. *J. Atmos. Sci.*, 63:1895–1909, 2006.

[8] R. T. Merrill and Christopher S. Velden. A three-dimensional analysis of the outflow layer of supertyphoon Flo (1990). *Mon. Wea. Rev.*, 124:47–63, 1996.

[9] J. Molinari, D. Knight, M. Dickinson, D. Vollaro, and S. Skubis. Potential vorticity, Easterly Waves, and Eastern Pacific tropical cyclogenesis. *Mon. Wea. Rev.*, 125:2699–2708, 1997.

[10] J. Molinari, S. Skubis, and D. Vollaro. External influences on hurricane intensity. Part III: Potential vorticity structure. *J. Atmos. Sci.*, 52:3593–3606, 1995.

[11] Y. Noh, W.-G. Cheon, S.-Y. Hong, and S. Raasch. Improvement of the K-profile model for the planetary boundary layer based on large eddy simulation data. *Bound. Lay. Met.*, 107:401–427, 2003.

[12] David S. Nolan. What is the trigger for tropical cyclogenesis? *Aust. Meteorol. Mag.*, 56:241–266, 2007.

[13] O. Pauluis, A. Czaja, and R. Korty. The global atmospheric circulation in moist isentropic coordinates. *J. Climate*, 23:3077–3093, 2010.

[14] O. M. Pauluis, T. Shaw, and F. Laliberte. A statistical generalization of the transformed eulerian-mean circulation for an arbitrary vertical coordinate system. *J. Atmos. Sci.*, 68:1766–1783, 2011.

[15] Olivier Pauluis, Arnaud Czaja, and Robert Korty. The global atmospheric circulation on moist isentropes. *Science*, 321(5892):1075–1078, 2008.

[16] R. Rotunno and K. A. Emanuel. An air-sea interaction theory for tropical cyclones. Part II: Evolutionary study using a nonhydrostatic axisymmetric numerical model. *J.Atmos.Sci.*, 44:542–561, 1987.

[17] C. M. Rozoff, D. S. Nolan, J. P. Kossin, F. Zhang, and J. Fang. The roles of an expanding wind field and inertial stability in tropical cyclone secondary eyewall formation. *J. Atmos. Sci.*, 69:2621–2643, 2012.

[18] W. H. Schubert and B. T. Alworth. Evolution of potential vorticity in tropical cyclones. *Quart. J. Roy. Meteor. Soc.*, 113:147–162, 1987.

[19] K.-M. Xu and K. A. Emanuel. Is the tropical atmosphere conditionally unstable? *Mon. Wea. Rev.*, 117:1471–1479, 1989.